coatings

MDPI

Article

Fabrication of Microalloy Nitrided Layer on Low Carbon Steel by Nitriding Combined with Surface Nano-Alloying Pretreatment

Jian Sun [1,*] and Quantong Yao [2]

[1] Department of Materials Science and Engineering, Hefei University of Technology, Hefei 230009, China
[2] Key Laboratory of Electromagnetic Processing of Materials, Ministry of Education, Northeastern University, Shenyang 110819, China; tongtong282@126.com
* Correspondence: sunjian@hfut.edu.cn; Tel.: +86-551-6290-4557

Academic Editor: Yilei Zhang
Received: 14 October 2016; Accepted: 8 November 2016; Published: 17 November 2016

Abstract: Surface mechanical attrition treatment (SMAT) is an effective method to accelerate the nitriding process of metallic materials. In this work, a novel technique named surface nano-alloying (SNA) was developed on the basis of surface mechanical attrition treatment, which was employed as a pretreatment for the nitriding of low carbon steel materials. The microstructure and surface properties of treated samples were investigated by SEM, XRD, TEM and the Vickers hardness test. Experimental results showed that a surface alloying layer (Cr element) of about 10–20 μm in thickness was formed on the low carbon steel sample after the surface nano-alloying treatment. After nitriding for the SNA sample, a complex compound layer composed of $Fe_{2-3}N$, FeCr and Cr_2N phases was fabricated. Moreover, the thickness of this compound layer was about 50 μm. Meanwhile, both the surface hardness and wear resistance of the SNA nitrided sample are better that those of the SMAT nitrided sample. This work offers a new approach for improving the nitriding process of steel materials.

Keywords: surface mechanical attrition treatment; surface nano-alloying; nitriding; diffusion; surface properties

1. Introduction

Surface mechanical attrition treatment (SMAT) is an effective surface modification technique to improve the surface properties of metallic materials including hardness, wear and corrosion resistance by server plastic deformation [1–8]. Using SMAT, different microstructures can be obtained within the deformed surface layer through the depth from the treated surface to the strain-free matrix, i.e., from nano-sized grains to sub-micro-sized and micro-sized crystalline on a bulk material [1,3–6]. Previous studies showed that the atom diffusion ability on SMATed materials was significantly enhanced due to the formation of a large number of grain boundaries or other defects (vacancy, dislocation and interfaces) by SMAT [9–14]. For example, Tong and Zhang showed that the gaseous nitriding of a SMATed pure iron plate and the plasma nitriding of a SMATed AISI 304 stainless steel specimen were also achieved recently at 300 °C and 400 °C, respectively. These temperatures are evidently lower than those in conventional nitriding processes (500–550 °C) [9,10]. In addition, the experiment of chromizing behaviors of the SMATed steel sample showed that the formation temperature of chromium compounds was found to be much lower and the amount of chromium carbides was higher than those in the coarse-grained counterpart [11]. Moreover, the significantly enhanced aluminizing behaviors of a low carbon steel at temperatures far below the austenitizing temperature, with a nanostructured surface layer produced by surface mechanical attrition treatment, was found to show us that SMAT seems to be appropriate for enhancing the atom diffusion ability efficiently [12].

As we know, mechanical alloying (MA) is a well-established method to prepare metastable phases (such as supersaturated solid solutions) by energetic collisions in a ball mill [15]. Additionally, surface mechanical alloying (SMA) was developed based on MA to fabricate coatings on metallic materials via ball milling [16]. Recently, a novel surface technology named surface nano-alloying (SNA) was developed on the basis of SMAT to fabricate a nanocrystalline composite surface on metallic materials [17–21]. Commonly, a small amount of alloy powder was added to the chamber before the SMAT process. Subsequently, the impacts of the milling balls delivered particles from the powder charge and attached them to the surface. Furthermore, due to the formation of a large number of deformation-induced non-equilibrium grain boundaries, non-equilibrium excessive vacancies and other defects, such as dislocations, twins and lattice strains induced by SMAT, the surface becomes chemically active, which may promote interdiffusion between the alloy element and substrate. Ultimately, a composite surface including the supersaturated solid solution, intermetallic compound and amorphous phases can be formed by this method [22]. At present, this method has become a hot topic in the surface engineering field. For example, Du et al. showed that Ni powders were welded into the surface of iron plates by SMAT [22]. Révész et al. illustrated that Cu plates were coated mechanically with a mixture of Ti and Zr powders via a combination of deposition, wear, deformation and defect-enhanced diffusion processes [23].

In this paper, surface nano-alloying was employed as a pretreatment for a low carbon steel sample. Subsequently, the nitriding behaviors of the surface nano-alloying sample were investigated in comparison with those of original and SMATed samples.

2. Materials and Methods

A 20 steel plate (4 × 100 × 100 mm^3 in size) with chemical composition of (in wt.%): 0.2 C, 0.17 Si, 0.5 Mn, 0.25 Cr, 0.035 P (max.), 0.035 S (max.) and balance Fe, was used in the present study. The as-received sample was annealed at 950 °C for 1 h in vacuum to eliminate the effect of mechanical deformation and to obtain homogeneous coarse grains. Prior to surface nano-alloying, the specimens were machined and surface-polished with silicon carbide paper to grade 1200.

SNA was performed in a vacuum chamber as the schematic diagram of the experimental apparatus shown in Figure 1. GCr15 steel balls with a diameter of 4 mm and about 1 g Cr powders were placed at the bottom of the chamber. This chamber was vibrated by a generator with a frequency of 50 Hz. The balls generated mechanical attrition on the surface of iron plate, producing plastic deformation in the surface layer, and welding of the Ni powders onto the surface of sample. In this work, the sample was treated for 60 min. Subsequently, the samples were treated by plasma nitriding at 550 °C for 4 h. The processing of plasma nitriding was described in our previous work [24].

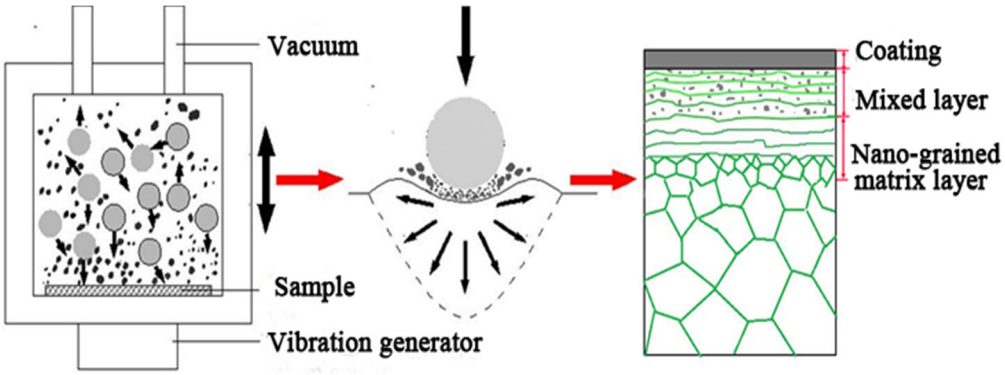

Figure 1. The schematic diagram of SNA processing.

The phase information of treated samples were analyzed by a X Pert Pro PW3040/60 X-ray diffractometer (XRD) (Panalytical, Almelo, The Netherlands) using Cu Kα radiation (40 kV, 40 mA).

Cross-sectional morphologies of various samples were observed by using Zeiss Ultra 55 scanning electron microscope (SEM) (Zeiss, Oberkochen, Germany). The element concentrations through the cross-section were analyzed by EDS (Zeiss, Oberkochen, Germany). Microstructure characterizations were also examined by using a Jeol-4000FX transmission electron microscope (TEM) (Jeol, Tokyo, Japan) with an operating voltage of 200 kV. The samples for TEM observation were prepared by grinding and mechanical polishing followed by ion-thinning at lower temperature.

Microhardness (HV) tests on the experimental samples were performed on a L101MVD model Vickers microhardness tester (Mitutoyo, Tokyo, Japan). The testing was carried out at a load of 25 g with duration of 10 s. Wear resistance tests were carried out on Optimol SRV®tribometer (Optimol, Berlin, Germany) with WC-6% Co ball. The duration of test is 30 min and the loads are 5 N, 15 N, 30 N, and 50 N, respectively. The wear volume loss was calculated by Archard formula.

3. Results and Discussion

3.1. Microstructure of SNA Sample

After SNA, the visual color of the sample surface changed from silver-white to gray-black, indicating the introduction of impurities into the surface layer during SNA. Figure 2 shows the cross-sectional SEM image and the corresponding EDS analysis of the SNA sample. It can be seen that the microstructure of the SNA sample were taken from different regions. Evidently, severe plastic deformation during the SNA process results in an inhomogeneous and non-uniform surface alloying layer (Cr element). The maximum thickness of the alloying layer can exceed 20 μm in some regions. In addition, a deformed layer (substrate) of about 100 μm in thickness can be found below the alloying layer.

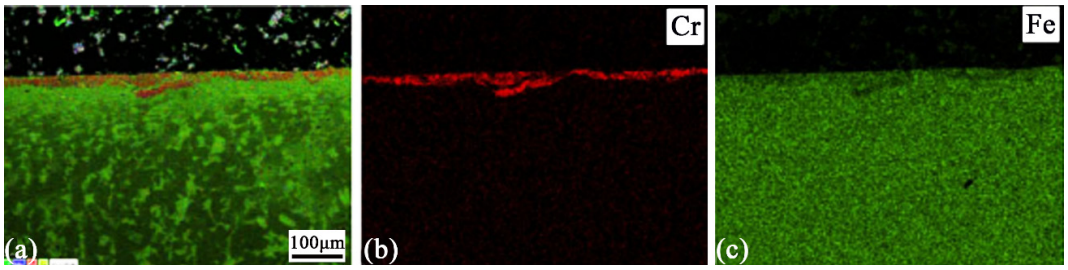

Figure 2. Cross-sectional morphology of SNA sample (**a**) and the corresponding EDS element mapping images: (**b**) Cr, (**c**) Fe.

3.2. Microstructure of SNA Sample after Nitriding

The image shown in Figure 3 is the cross-sectional SEM microstructure of the SNA sample after nitriding at 550 °C for 4 h, in comparison with that of the SMAT sample after nitriding at the same conditions. For the SMAT nitrided sample, the nitrided layer includes the compound layer, transition zone and diffusion layer from the surface to the inside, respectively, as shown in Figure 3a. The compound layer thickness in the SMAT nitrided sample is 30 μm. However, an obviously different microstructure was detected on the SNA nitrided sample. As shown in Figure 3b, it can be observed that a complex compound layer about 50 μm thick was formed on the SNA nitrided sample. Especially, the overall compound layer can be categorized into three parts from the top surface into the interior. The outermost layer is very dense, the thickness of which is about 20 μm. The middle layer displays a needle-like shape and the inner layer is not uniform. The formation of the complex compound layer may originate from the interdiffusion between nitrogen, chromium and ferrite atoms.

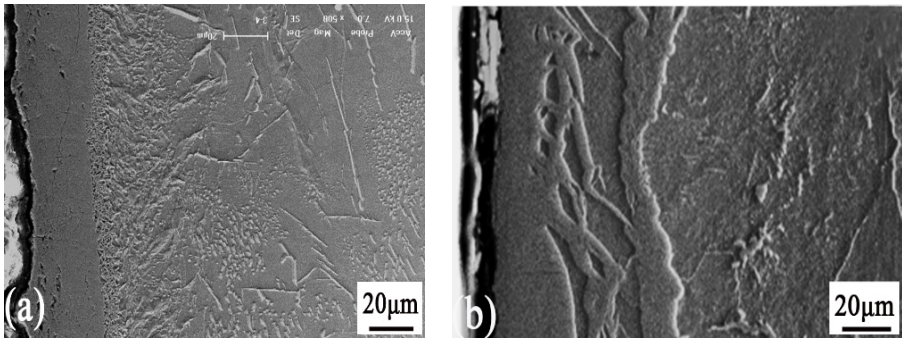

Figure 3. Cross-sectional SEM images of SMAT nitrided sample (**a**) and SNA nitrided sample (**b**).

To further investigate the phase information of the SNA nitrided sample, the XRD analysis was employed and its results are shown in Figure 4. It can be observed that the surface layer of the SMAT nitrided sample consists of $Fe_{2-3}N$ and Fe_4N phases. However, in the SNA sample nitrided under the same conditions, strong FeCr and Cr_2N phase diffraction peaks can be observed, indicating that interdiffusion may happen during the nitriding process. These results can be confirmed by the TEM observation and the corresponding selected area electron diffraction (SAED, shown in Figure 5). From the TEM results, it can be seen that the composition of the surface layer of the SNA nitrided sample was found to be composed of an ultrafine polycrystalline compound. The phases include $Fe_{2-3}N$, FeCr and Cr_2N, and these results are in agreement with the XRD analysis. As we know, SMAT can enhance the nitrogen diffusion ability in pure iron materials and result in significantly improved surface properties relative to those of the coarse-grain nitrided sample due to the "nano-effect". In this paper, the SNA method can not only offer the "nano-effect", but it also brings the alloy element into the nitrides, which may have a significant impact on the hardness and wear resistance, as will be shown later.

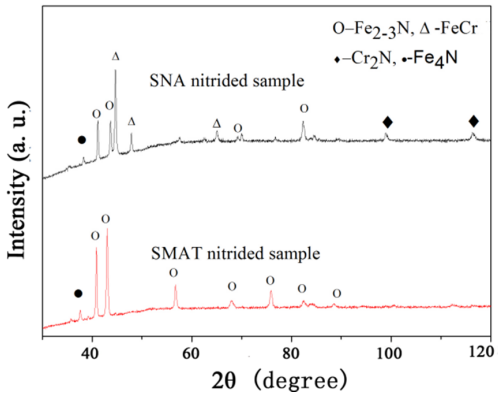

Figure 4. XRD pattern of two kinds of samples.

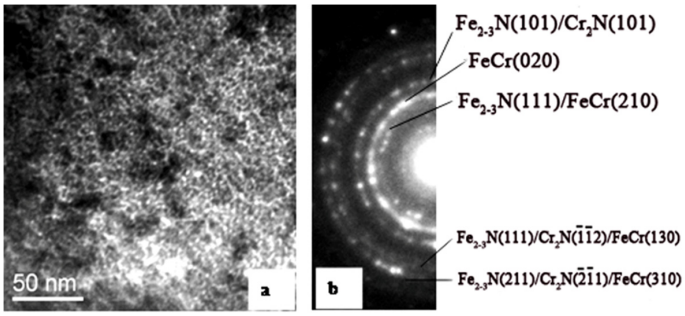

Figure 5. TEM observation (**a**) and corresponding SAED (**b**) of SNA nitrided sample.

3.3. Surface Properties of SNA Nitrided Sample

The variation of the hardness along the depth in the SNA sample nitrided at 550 °C is shown in Figure 6, in comparison with that of the SMAT sample nitrided in the same conditions. It should be noted that a hardness value of 1168 HV was obtained on the surface layer of the SNA nitrided sample, which is a significantly higher value than that recorded for the SMAT nitrided sample (846 HV). The variation of the hardness along the depth revealed the presence of a hardened surface layer, which was defined by the distance from the surface to the point where the microhardness was 50 HV higher than that in the matrix. This hardened surface layer is more than 350 μm in thickness for the SNA nitrided sample. In comparison, the hardness was approximately 846 HV at the surface and decreased sharply to the substrate value within 280 μm of the surface of the SMAT nitrided sample.

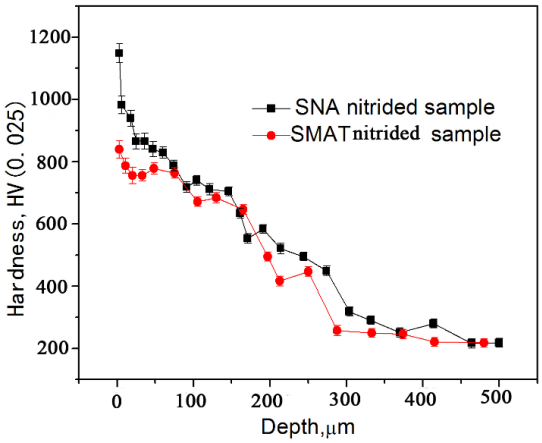

Figure 6. Hardness variations along the depth of both the SNA nitrided sample and the SMAT nitrided sample.

Measurements of volume losses of wear scars at various loads ranging from 5 to 50 N were performed on the SNA nitrided sample and the SMAT nitrided sample, respectively, as depicted in Figure 7. The wear volume loss values of both samples increased with the longer testing time, but the wear volume losses of the SNA nitrided sample were remarkably smaller than those of the SMAT nitrided sample for each sliding time. For example, the wear loss of the SNA nitrided sample was less than one half of that of the SMAT nitrided sample at load of 50 N. This observation indicates that the wear resistance of the SNA nitrided sample is better than that of the SMAT nitrided sample.

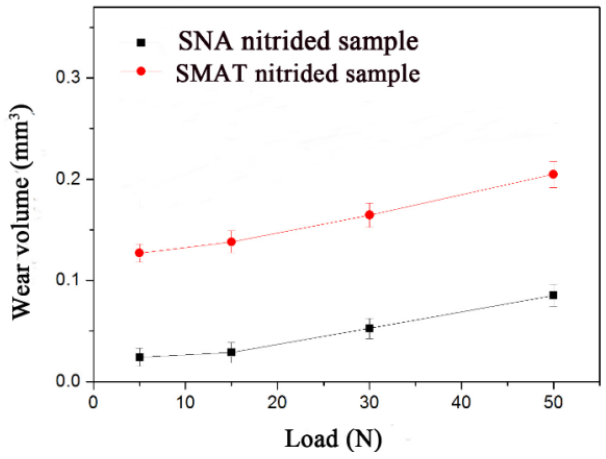

Figure 7. Variations in the wear volume losses with load of both the SNA nitrided sample and the SMAT nitrided sample.

4. Conclusions

The nitriding behavior of low carbon steel with a nano-alloying surface layer induced by SMAT with Cr powders was investigated in comparison with that of the SMAT sample after nitriding at the same conditions. The following conclusions were reached:

- After the surface nano-alloying treatment, a surface alloying layer (Cr element) of about 10–20 μm in thickness was formed on the low carbon steel sample. Additionally, a deformed substrate layer of about 100 μm can be detected at the subsurface.
- After nitriding for the SNA sample, a complex compound layer composed of $Fe_{2-3}N$, FeCr and Cr_2N phases was fabricated. Moreover, the thickness of this compound layer is about 50 μm.
- Both the surface hardness and wear resistance of the SNA nitrided sample are better than those of the SMAT nitrided sample.

Acknowledgments: This work was supported by the Fundamental Research Funds for the Central Universities (JZ2014HGBZ0042, JZ2016HGTA0702 and 2014HGQC0005), and the Anhui Provincial Natural Science Foundation (JZ2015AKZR0655).

Author Contributions: Jian Sun conceived and designed the experiments; Jian Sun performed the experiments; Jian Sun and Quantong Yao analyzed the data; Jian Sun wrote the paper.

Conflicts of Interest: The authors declare no conflict of interest.

References

1. Lu, K.; Lu, J. Surface nanocrystallization (SNC) of metallic materials: Presentation of the concept behind a new approach. *J. Mater. Sci. Technol.* **1993**, *15*, 193–197.
2. Tao, N.R.; Wang, Z.B.; Tong, W.P.; Sui, M.L.; Lu, J.; Lu, K. An investigation of surface nanocrystallization mechanism in Fe induced by surface mechanical attrition treatment. *Acta Mater.* **2002**, *50*, 4603–4616. [CrossRef]
3. Wu, X.; Tao, N.R.; Hong, Y.; Xu, B.; Lu, J.; Lu, K. Microstructure and evolution of mechanically-induced ultrafine grain in surface layer of Al-alloy subjected to USSP. *Acta Mater.* **2002**, *50*, 2075–2084. [CrossRef]
4. Yong, X.P.; Liu, G.; Lu, K.; Lu, J. Characterization and properties of nanocstructured surface layer in low carbon steel subjected to surface mechanical attrition. *J. Mater. Sci. Technol.* **2003**, *19*, 1–4.
5. Roland, T.; Retraint, D.; Lu, K.; Lu, J. Enhanced mechanical behavior of a nanocrystallised stainless steel and its thermal stability. *Mater. Sci. Eng. A* **2007**, *445–456*, 281–288. [CrossRef]
6. Wang, Y.M.; Pan, D.; Lu, K.; Hemkeri, K.J. Microsample tensile testing of nanocrystalline copper. *Scr. Mater.* **2003**, *48*, 1581–1586. [CrossRef]
7. Amanov, A.; Cho, I.S.; Kim, D.E.; Pyun, Y.S. Fretting wear and friction reduction of CP titanium and Ti-6Al-4V alloy by ultrasonic nanocrystalline surface modification. *Surf. Coat. Technol.* **2012**, *27*, 135–142. [CrossRef]
8. Chang, H.W.; Kelly, P.M.; Shi, Y.N.; Zhang, M.X. Thermal stability of nanocrystallized surface produced by surface mechanical attrition treatment in aluminum alloys. *Surf. Coat. Technol.* **2012**, *26*, 3970–3980. [CrossRef]
9. Tong, W.P.; Tao, N.R.; Wang, Z.B.; Lu, J.; Lu, K. Nitriding iron at lower temperatures. *Science* **2003**, *299*, 686–688. [CrossRef] [PubMed]
10. Zhang, H.W.; Wang, L.; Hei, Z.K.; Liu, G.; Lu, J.; Lu, K. Low-temperature plasma nitriding of AISI 304 stainless steel with nano-structured surface layer. *Z. Metallkunde* **2003**, *94*, 1143–1147. [CrossRef]
11. Wang, Z.B.; Lu, J.; Lu, K. Chromizing behaviours of a low carbon steel processed by means of surface mechanical attrition treatment. *Acta Mater.* **2005**, *53*, 2081–2089. [CrossRef]
12. Si, X.; Lu, B.; Wang, Z.B. Aluminizing low carbon steel at lower temperatures. *J. Mater. Sci. Technol.* **2009**, *25*, 433–436.
13. Wang, Z.B.; Tao, N.R.; Tong, W.P.; Lu, J.; Lu, K. Diffusion of chromium in nanocrystalline iron produced by means of surface mechanical attrition treatment. *Acta Mater.* **2003**, *51*, 4319–4329. [CrossRef]
14. Tong, W.P.; Liu, C.Z.; Wang, W.; Tao, N.R.; Wang, Z.B.; Zuo, L.; He, J.C. Gaseous nitriding of iron with a nanostructured surface layer. *Scr. Mater.* **2007**, *57*, 533–536. [CrossRef]

15. Takacs, L.; Torosyan, A.R. Surface mechanical alloying of an aluminum plate. *J. Alloys Compd.* **2007**, *434*, 686–688. [CrossRef]
16. Baláž, P.; Takacs, L.; Ohtani, T.; Mack, D.E.; Boldižárová, E. Properties of a new nanosized tin sulphide phase obtained by mechanochemical route. *J. Alloys Compd.* **2002**, *337*, 76–82. [CrossRef]
17. Li, W.; Wang, X.D.; Meng, Q.P.; Rong, Y.H. Interdiffusion of alloying elements in nanocrystalline Fe-30 wt.% Ni alloy during surface mechanical attrition treatment and its effect on $\alpha \rightarrow \gamma$ transformation. *Scr. Mater.* **2008**, *59*, 344–347. [CrossRef]
18. Meng, Y.F.; Shen, Y.F.; Chen, C.; Li, Y.C.; Feng, X.M. Effects of Cu content and mechanical alloying parameters on the preparation of W-Cu composite coatings on copper substrate. *J. Alloys Compd.* **2014**, *585*, 368–375. [CrossRef]
19. Wen, L.; Wang, Y.M.; Zhou, Y.; Guo, L.X.; Qu, J.H. Iron-rich layer introduced by SMAT and its effect on corrosion resistance and wear behavior of 2024 Al alloy. *Mater. Chem. Phys.* **2011**, *126*, 301–309. [CrossRef]
20. Romankov, S.; Hayasaka, Y.; Kasai, E.; Yoon, J.M. Fabrication of nanostructured Mo coatings on Al and Ti substrates by ball impact cladding. *Surf. Coat. Technol.* **2010**, *205*, 2313–2321. [CrossRef]
21. Romankov, S.; Sha, W.; Kaloshkin, S.D.; Kaevitser, K. Fabrication of Ti-Al coatings by mechanical alloying method. *Surf. Coat. Technol.* **2006**, *201*, 3235–3245. [CrossRef]
22. An, Y.L.; Du, H.Y.; Wei, Y.H.; Wang, N.; Hou, L.F.; Lin, W.M. Interfacial structure and mechanical properties of surface iron–nickel alloying layer in pure iron fabricated by surface mechanical attrition alloy treatment. *Mater. Des.* **2013**, *46*, 427–433. [CrossRef]
23. Revesz, A.; Takacs, L. Coating a Cu plate with a Zr-Ti powder mixture using surface mechanical attrition treatment. *Surf. Coat. Technol.* **2009**, *203*, 3026–3031. [CrossRef]
24. Sun, J.; Tong, W.P.; Zhang, H.; Zuo, L.; Wang, Z.B. Low-temperature plasma nitriding of titanium layer on Ti/Al clad sheet. *Mater. Des.* **2013**, *47*, 408–415. [CrossRef]